Applied Radiation and Isotopes 88 (2014) 50–54

Contents lists available at ScienceDirect

Applied Radiation and Isotopes

journal homepage: www.elsevier.com/locate/apradiso

Design, construction and application of a neutron shield for the treatment of diffuse lung metastases in rats using BNCT

A. Razetti [a], R.O. Farías [a,b,c], S.I. Thorp [c], V.A. Trivillin [b,c], E.C.C. Pozzi [c], P. Curotto [c], A.E. Schwint [b,c], S.J. González [b,c,*]

[a] Universidad Favaloro, FICEN, Av. Belgrano 1723 (1093), C.A.B.A., Buenos Aires, Argentina
[b] CONICET, Av. Rivadavia 1917 (1033), C.A.B.A., Córdoba, Argentina
[c] Comisión Nacional de Energía Atómica (CNEA), Av. Gral Paz 1499 (1650), Buenos Aires, Argentina

HIGHLIGHTS

- A practical shielding device that comfortably houses a rat is presented.
- The shield allows a uniform and useful dose in the rat thoracic area.
- A novel computational dosimetry in animals based on Multicell is presented.
- Experimental characterization evidences the good performance of the shield.
- An irradiation based on a diffuse lung metastases model in rats was performed.

ARTICLE INFO

Available online 27 December 2013

Keywords:
Lung cancer
Multiple metastatic disease
MCNP
Neutron attenuation
Computational dosimetry

ABSTRACT

A model of multiple lung metastases in BDIX rats is under study at CNEA (Argentina) to evaluate the feasibility of BNCT for multiple, non-surgically resectable lung metastases. A practical shielding device that comfortably houses a rat, allowing delivery of a therapeutic, uniform dose in lungs while protecting the body from the neutron beam is presented. Based on the final design obtained by numerical simulations, the shield was constructed, experimentally characterized and recently used in the first in vivo experiment at RA-3.

© 2013 Elsevier Ltd. All rights reserved.

1. Introduction

Multiple metastatic lung cancer is different from localized tumors mainly because it cannot be segregated from healthy tissue, as malignant cells are spread all through it. Therefore, the gross tumor volume (GTV) cannot be segmented in a CT or X-ray image in order to selectively treat tumor cells with radiotherapy, at least not with the conventional irradiation techniques. This makes it tempting for radiobiologists and other scientists to explore and apply new techniques in this field, such as the so-called boron neutron capture therapy (BNCT). BNCT has been applied in Japan to treat mesotheliomas and localized lung tumours using external collimated neutron beams (Suzuki et al., 2008, 2012). In addition, the BNCT group of the Comisión Nacional de Energía Atómica of Argentina (CNEA) is studying the feasibility of using this irradiation technique to treat surgically untreatable multiple lung metastases locally confined without pleural invasion. The ultimate objective of the project is to develop a clinical protocol that would involve explanting tumor-bearing lungs, treat them with BCNT, and then reimplant the organs into the patient. Within this context, and based on previous work of Altieri et al. (2006), Bakeine et al. (2009), Bortolussi et al. (2011a, 2011b), the radiobiology group at CNEA has designed a preclinical protocol based on a colon carcinoma multiple lung metastases model in BDIX rats (Trivillin et al., this issue). The animals treated with BNCT are evaluated for radiotoxic and tumor control effects, and finally the feasibility of the technique will be assessed. Animal irradiations are carried out in the biomedical facility of the RA-3 reactor (CNEA) (Miller et al., 2009). The facility is located in the thermal column of the reactor, 2 m far from the core pool. The irradiation cavity, 15 cm wide, 20 cm long and 10 cm high, is completely surrounded by graphite blocks, and the neutron flux inside the cavity can be described as a uniform, quasi-isotropic thermal flux of about 10^{10} n cm^{-2} s^{-1}.

The aim of this work was to design and build a practical and manageable shielding device capable of comfortably housing a rat during a therapeutic irradiation process at RA-3 while protecting the body from the neutron beam, as well as allowing the delivery of a therapeutically useful and uniform dose in the lungs. Based on the final design obtained by numerical simulations, the shielding

* Corresponding author at: Subgerencia Instrumentación y Control, Comisión Nacional de Energía Atómica (CNEA), Avenida General Paz 1499 (1650), San Martín, Provincia Buenos Aires, Argentina. Tel.: +54 11 6772 7865; fax: +54 11 6772 7611.
E-mail address: srgonzal@cnea.gov.ar (S.J. González).

0969-8043/$ - see front matter © 2013 Elsevier Ltd. All rights reserved.
http://dx.doi.org/10.1016/j.apradiso.2013.12.021

device was constructed and experimentally characterized. Given the adequate dosimetry results obtained from measurements, the first experiment with living animals was carried out.

2. Materials and method

The program used throughout the design process to simulate the particle transport in the shield and computationally characterize the neutron flux distribution for the proposed configurations was the Monte Carlo transport code MCNP (X-5 Monte Carlo Team, 2008). Two MCNP models of the RA-3 facility were used: (1) a simplified representation that allows for rapid screening of different configuration set-ups while deriving quite accurate results with short time simulations (Farías et al., 2009), and (2) a complete source model that mimics the exact geometry and materials of the whole reactor and biomedical facility is used to obtain more accurate results at the cost of increasing simulation times (Bortolussi et al., 2011a, 2011b).

3. Design goals

In view of the objectives proposed in the preclinical protocol and the limited dimensions of the irradiation cavity, the requirements of the shield are as follows:

- the geometry must be as simple as possible to easily introduce and remove the shielding device from the irradiation tray;
- the animal positioning must be comfortable, practical and repeatable;
- it should allow the delivery of a uniform and therapeutically useful dose in the rat thoracic area while keeping the dose delivered to other organs at low values (Fig. 1).

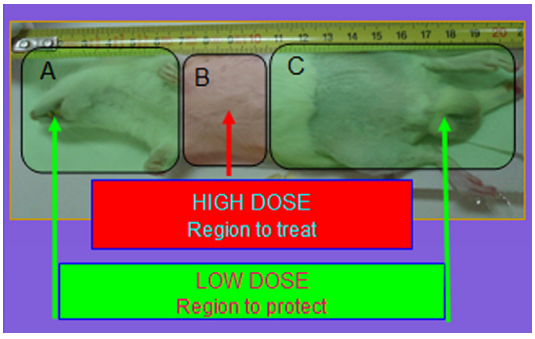

Fig. 1. Ideal dose distribution over the rat's anatomy. Regions A and C are protected by the shield while region B is the volume to treat.

4. Materials and geometry

The attenuating material readily available at CNEA to build the shielding device was fine powder of ^{6}Li-enriched lithium carbonate (Li_2CO_3). Previous experience of the group in constructing this kind of devices showed that the powder can be compressed between two thin acrylic walls without introducing significant undesired radiation contamination. The starting design was a Li_2CO_3-filled 2 mm acrylic double walled cylinder of 20 cm length. To determine a suitable amount of the attenuating material, Li_2CO_3 thicknesses from 0.6 to 1.2 cm were explored and assessed based on neutron flux evaluations. Once the appropriate thickness of the attenuating material was determined, the second step was to define the dimensions of the shielding device and final geometry in keeping with the design goals mentioned above. After some assays and practical considerations, it was decided to give the device the shape of a longitudinally cut cylinder open at one end, which is then closed with a separate lid. The animal is in turn positioned on a separate acrylic holder so that it can easily be inserted into and removed from the shielding.

Different shapes of collimated apertures to expose the lung area to neutrons were proposed: (a) a conical upper inward collimator centered on the lung area, designed to avoid the direct neutron flux on the tangential organs, (b) a rectangular collimator with a lateral 135° aperture designed to maximize the neutron flux homogeneity in the treatment area while minimizing the dose to the spinal cord and peripheral organs, and (c) a rectangular collimator with a lateral 180° aperture.

The comparison between different configurations was performed on the basis of the dose distribution obtained in the rat's organs at risk (OAR) as well as in the planning target volume (PTV). Since for multiple pulmonary metastases malignant cells cannot be segregated, at least not on a macro scale, the PTV encompassed the entire lung volume. Computational simulations were carried out using an analytic model of the rat.

5. Detailed dosimetrical analysis

In order to define the final aperture and design of the shielding device, a more specific and realistic dosimetrical analysis was performed. Fig. 2 depicts the rat model used in the final design

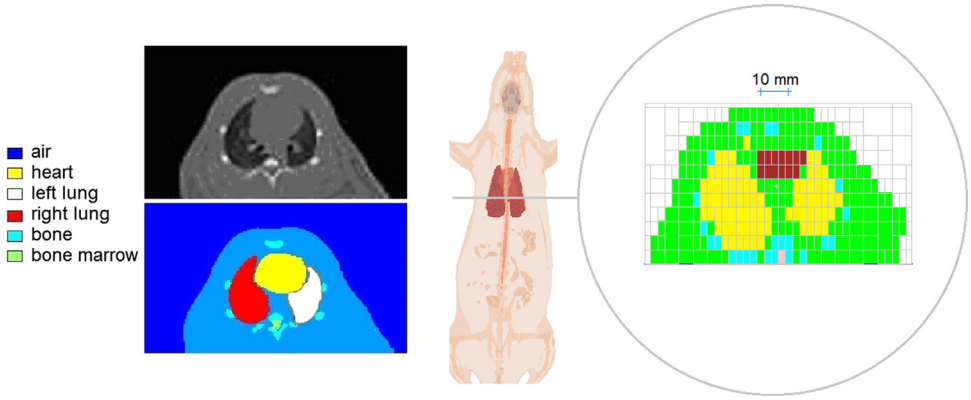

Fig. 2. (left) Thoracic CT image of a rat before and after organs' segmentation, (right) coronal and axial planes of the voxelized model of the rat drawn with Moritz 3D® and MCNP plotter, respectively.

process, obtained with the MultiCell algorithm developed in CNEA (Argentina) (Farias and González, 2012). It consists of the segmentation and voxelization of a set of 256 CT images from a real rat. Note that simulating the animal's anatomy this way has the benefit that both the size and shape of the different structures can be accurately described.

The main organs at risk considered for dose analysis were selected based on the level of exposure. Dose limits were taken from QUANTEC (2010) publication for conventional radiotherapy, and when necessary, translated into single fraction doses using the LQ model. The selected OARs and the corresponding dose limits are listed in Table 1.

Apart from the main OARs, liver, brain and kidneys were also considered for dose analysis. Although inside the shielding the neutron flux is expected to be almost two orders of magnitude lower compared to the zone outside the shielding for the three selected apertures, normal tissues should receive a dose as low as possible (ALARA concept).

The weighted doses, that will be expressed in Gy_w, were calculated employing previously reported RBE and CBE factors, i.e. CBE factor of 1.4 for lung (Liu Kiger et al., 2008), CBE factor of 3.8 for tumor (Coderre and Morris, 1999), CBE factor of 2.5 for skin (González et al., 2004), and an RBE factor of 3 for all tissues (Liu Kiger et al., 2008). In addition, the boron concentration values for each organ reported in Trivillin et al. (this issue)for three different protocols involving BPA and/or GB-10, were used to analyze the dosimetry in the animal.

Table 1
Main OARs considered for dose analysis and corresponding dose limits.

Organ at risk	Dose constraint
Healthy lung	$D_{max} < 18.6$ Gy $D_{mean} < 9.1$ Gy $V_{9.1} < 30\%$
Heart	$D_{max} < 10.4$ Gy $V_{9.4} < 10\%$
Esophagus	$D_{mean} < 10.4$ Gy
Bone marrow	$D_{max} < 13$ Gy

6. Shield construction: Final considerations

After the optimum computational shielding device design was achieved, a few minor adjustments were made in order to make the device easier to build. They mainly consisted of adjusting some Li_2CO_3 and acrylic thicknesses and the way the acrylic pieces would fit in together. Once the acrylic double walled structure was constructed, it was carefully filled with Li_2CO_3. Since the attenuating material was in the form of a very fine powder, it was quite difficult to manage and compact without leaving free spaces. The two pieces of the shield, i.e. the cut cylinder and the lid, were separately weighed before and after filling in order to obtain the net mass of Li_2CO_3 used in each structure. The free volume inside each piece (i.e. the space left between the acrylic walls for the Li_2CO_3) was calculated with MCNP. Then, based on the net Li_2CO_3 masses and volume results, average densities of the air and Li_2CO_3 mixtures were estimated. Then, new materials consisting of a mixture of air and Li_2CO_3 were considered for final simulations with MCNP, in order to compare the computational results with those obtained from the experimental characterization of the built device.

7. Experimental characterization

Two neutron activation experiments were performed comprising an *in air* (i.e. using an empty shield) and *in an acrylic rat phantom* (Fig. 3) characterization. As shown in Fig. 4, the first

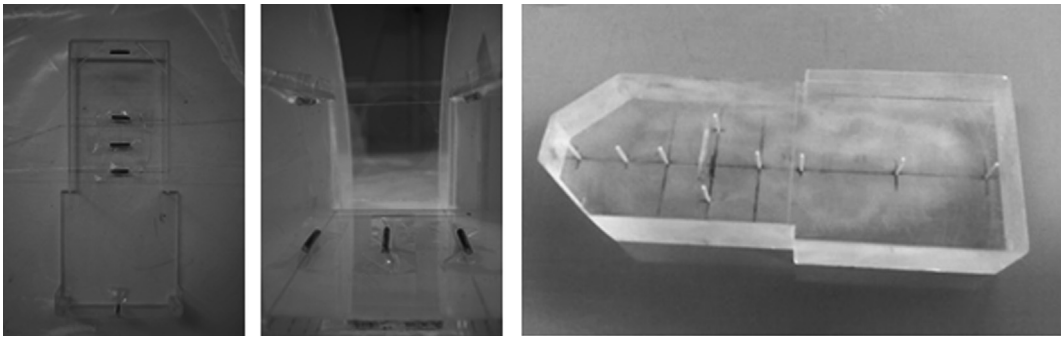

Fig. 3. (a) Position of the seven Cu–Au wires as used in the *in air* characterization, (left) acrylic holder, (right) shield aperture. (b) Acrylic rat phantom used for *in phantom* characterization. Nine out of eleven activation wires were introduced in the acrylic holes. The remaining wires were horizontally positioned at the top and bottom of the phantom at the thoracic area (i.e., heart and spinal cord of the animal, respectively).

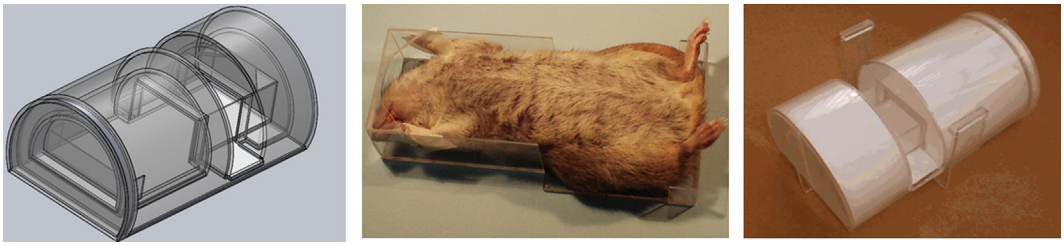

Fig. 4. (left) Digital reconstruction of the shield in Solid Works®, (center) Rat positioned on the acrylic holder for irradiation, (right) Built shielding device.

experiment set-up involved an empty shield and comprised measurements of the thermal neutron flux using seven activation wires composed of copper alloyed with 1.55% gold by weight (Cu–Au), set on relevant positions of the shield. The second activation experiment was carried out using the acrylic rat phantom inserted in the shield. For this case, eleven activation Cu–Au wires were distributed along the phantom, as depicted in Fig. 3. In both cases, the shield was placed at the facility in the same way as planned for the experiments with animals. Gammas from the activated wires were measured using a high-purity germanium detector previously calibrated using a commercial Europium source of certified activity (Certificate of calibration No. 76044A-440, Eckert & Ziegler Analytics, Inc., October 23, 2007. Analytics maintain traceability to National Institute of Standards and Technology).

The two experimental set-ups were simulated in MCNP and the neutron flux in each wire was thus estimated and compared with measurements.

8. Results

Results obtained regarding the study of the pure Li_2CO_3 (δ=2.11 g cm^{-3}) attenuation capability as a function of the thickness of the material reveals that the neutron flux decreases one order of magnitude for each 0.2 cm increase in the Li_2CO_3thickness.

Combining these results and design goals, Li_2CO_3 thicknesses between 0.8 and 0.9 cm were considered for the whole device except for the lid for which a 1 cm material thickness was selected. Regarding the aperture to allow neutrons to reach the thorax of the rat, a 180°-opened window proved most suitable in terms of the detailed dosimetry analysis. The final thickness for the acrylic walls in the body of the shield and lid was 0.3 cm, while the rest of the acrylic pieces were 0.2 cm thick. The holder is 0.3 cm thick, and its supporting pieces are 0.1 cm thick.

From left to right Fig. 4 shows a digital reconstruction of the final shield design (only the acrylic pieces), the rat positioned on the acrylic holder for irradiation, and the built shielding device. As can be noticed the design immobilizes the rodent and allows a convenient and repeatable positioning for irradiation. The shielding device, built according to the final design, shows an acrylic structure on both sides of the cut cylinder used to easily introduce and remove the shield from the irradiation tray.

The density of the mixture material in the body of the shield and lid were found to be 0.976 and 0.852 g cm^{-3}, respectively. This corresponds to 46% Li_2CO_3 and 54% air for the body and 40% Li_2CO_3 and 60% air for the lid.

Detailed dose distributions in the rat OARs and PTV were obtained using the final shield geometry and the voxelized model of the animal. As a representative case, boron concentration values reported in Trivillin et al. (this issue) for BPA (46.5 mg 10B/kg) i.p. boron administration protocol were used in the example. Cumulative dose–volume histograms for the most relevant OARs and PTV are shown in Fig. 5 (the dose for the other analyzed organs was well below the considered limits).

The wide therapeutic window of about 10 Gy_w can be observed between the healthy lungs and the PTV.

Fig. 6a and b presents the results of the neutron flux characterization using the empty shield and the shield holding the acrylic rat phantom. Experimental and computational results matched within an acceptable error. Computational data accurately follows the general behavior of the experimental results in both characterizations; however, the calculated neutron fluxes in the in phantom experiment at the region B (thoracic area) underestimates between 2 and 30% the measurements (average 20%). A more detailed analysis regarding the air–Li_2CO_3 mixture material homogeneity could shed light on this matter. Finally, experimental results evidence the good performance of the shield; the in air characterization derived high and uniform neutron flux values at the shielding aperture and sufficiently low values inside the device. In addition, the acrylic rat phantom-based experiment showed a high enough ($\sim 10^9$ n cm^2 s^{-1}) and homogenous neutron flux in the volume to treat (region B) with a significant neutron flux reduction, up to 10^7 n cm^2 s^{-1}, in the zones under the Li_2CO_3 (regions A and C).

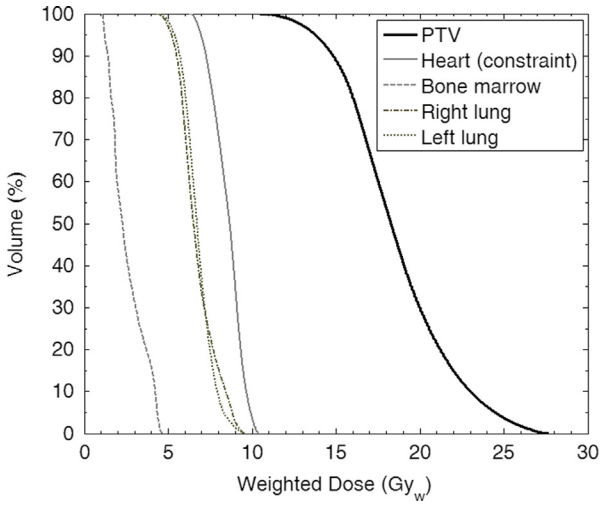

Fig. 5. Cumulative dose–volume histograms for different organs in the rat model.

9. Conclusions

A practical and easy to handle shield was achieved, with the capability of allowing a uniform and therapeutically useful dose in the rat thoracic area while protecting effectively the rest of the

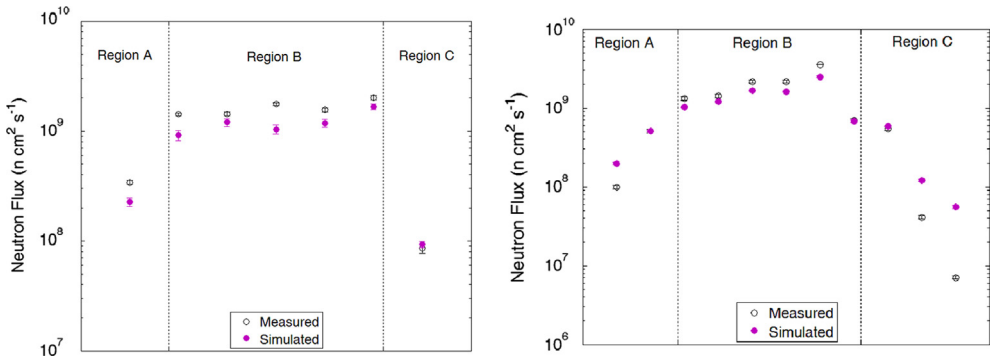

Fig. 6. Experimental and computational results of the neutron flux characterization for the final shield geometry corresponding to the (a) in air and (b) in an acrylic rat phantom set-ups. Logarithmic scales have been applied to the vertical axis.

animal's body, during a half an hour irradiation at the RA-3 biomedical facility. Given the acceptable agreement between the experimental and computational results from the in air and in phantom characterizations, numerical simulations can then be trusted to derive the dosimetry and compute treatment times for the experiments involving the irradiation of living animals. A treatment planning software has been developed to help radiobiologists to determine the duration of the experiments according to the dose constraints and the prescribed control dose in the target.

As a result of this work, the first irradiation experiment within the context of the preclinical protocol based on a colon carcinoma diffuse lung metastases model in BDIX rats has recently been carried out.

Acknowledgments

The authors are deeply grateful to Dr. David Nigg for providing them with the ^{6}Li-enriched lithium carbonate powder used for the shield built in the present work.

References

Altieri, S., Bortolussi, S., Bruschi, P., Fossati, F., Vittor, K., Nano, R., Facoetti, A., Chiari, P., Bakeine, J., Clerici, A., Ferrari, C., Salvucci, O., 2006. Boron absorption imaging in rat lung colon adenocarcinoma metastases. J. Phys. Conf. Ser., 41.

Bakeine, G.J., Di Salvo, M., Bortolussi, S., Stella, S., Bruschi, P., Bertolotti, A., Nano, R., Clerici, A., Ferrari, C., Zonta, C., Marchetti, A., Altieri, S., 2009. Feasibility study on the utilization of boron neutron capture therapy (BNCT) in a rat model of diffuse lung metastases. Appl. Radiat. Isot. 67 (7–8), S332–S335.

Bortolussi, S., Bakeine, J.G., Ballarini, F., Bruschi, P., Gadan, M.A., Protti, N., Stella, S., Clerici, A., Ferrari, C., Cansolino, L., Zontad, C., Zontad, A., Nanoe, R., Altieri, S., 2011a. Boron uptake measurements in a rat model for Boron Neutron Capture Therapy of lung tumours 69 (2), 394–398.

Bortolussi, S., Pinto, J.M., Thorp, S.I., Farias, R.O., Soto, M.S., Sztejnberg, M., Pozzi, E.C. C., González, S.J., Gadan, M.A., Bellino, A.N., Quintana, J., Altieri, S., Miller, M., 2011b. Simulation of the neutron flux in the irradiation facility at RA-3 reactor. Appl. Radiat. Isot. 69 (12), 1924–1927.

Coderre, J.A., Morris, G.M., 1999. The radiation biology of boron neutron capture therapy. Radiat. Res. 151, 1–18.

Farías, R.O., González, S.J., Bellino, A., Bortolussi, S., Sztenjberg, M., Pinto, J., Thorp, S. I., Gadan, M.A., Soto, M.S., Pozzi, E.C.C., Nigg, D.W., Schwint, A.E., Heber, E.M., Trivillin, V.A., Zarza, L., Estryk, G., Miller, M., 2009. Computational modeling for human extracorporeal irradiations using the Argentine BNCT facility of the RA-3 reactor. In: Proceedings of the Young Researchers Boron Neutron Capture Therapy Meeting, Mainz, Germany.

Farias, R.O., González, S.J., 2012. MultiCell model as an optimized strategy for BNCT treatment planning. In: Abstracts book of the 15th International Congress on Neutron Capture Therapy, Tsukuba, Japan.

González, S.J., Bonomi, M.R., Santa Cruz, G.A., Blaumann, H.R., Calzetta Larrieu, O.A., Menendez, P., et al., 2004. First BNCT treatment for a skin melanoma in Argentina: dosimetric analysis and clinical outcome. Appl. Radiat. Isot. 61, 1101–1105.

Liu Kiger, J., Kiger III, W.S., Riley, K.J., Binns, P.J., Patel, H., Hopewell, J.W., et al., 2008. Functional and histological changes in rat lung after BNCT irradiation. Radiat. Res. 170, 60–69.

Miller, M., Quintana, J., Ojeda, J., Langan, S., Thorp, S., Pozzi, E.C.C., Sztejnberg, M., Estryk, G., Nosal, R., Saire, E., Agrazar, H., Graiño, F., 2009. New irradiation facility for biomedical applications at the RA-3 reactor thermal column. Appl. Radiat. Isot. 67 (7–8), S226–S229.

QUANTEC, 2010. Int. J. Radiat. Oncol. Biol. Phys 76 (3).

Suzuki, M., Endo, K., Satoh, H., Sakurai, Y., Kumada, H., Kimura, H., Shinichiro Masunaga, Yuko, Kinashi, Kenji, Nagata, Akira, Maruhashi, Koji Ono, 2008. A novel concept of treatment of diffuse or multiple pleural tumors by boron neutron capture therapy (BNCT). Radiot. Oncol. 88, 192–195.

Suzuki, M., Suzuki, O., Sakurai, Y., Tanaka, H., Kondo, N., Kinashi, Y., Masunaga, Shinichiro, Maruhashi, Akira, Ono, Koji, 2012. Reirradiation for locally recurrent lung cancer in the chest wall with boron neutron capture therapy (BNCT). Int. Cancer Conf. J. , http://dx.doi.org/10.1007/s13691-012-0048-8.

V.A. Trivillin, M.A. Garbalino, L. Colombo, S.J. González, R.O. Farias, A. Monti Hughes, E.C.C. Pozzi, S. Bortolussi, et al., Biodistribution of the boron carriers boronophenylalanine (BPA) and/or decahydrodecaborate (GB-10) for Boron Neutron Capture Therapy (BNCT) in an experimental model of lung metastases. In: 15th International Congress on Neutron Capture Therapy, this issue.

X-5 Monte Carlo Team, MCNP—A General Monte Carlo N-Particle Transport Code, Version 5—Volume I: Overview and Theory, LA-UR-03-1987, Los Alamos National Laboratory, Revised 2/2008 (2008).